Physics Letters A ••• (••••) •••–•••

Contents lists available at ScienceDirect

Physics Letters A

www.elsevier.com/locate/pla

Liquid flow over a substrate structured by seeded nanoparticles

A.V. Lukyanov

Department of Mathematics, University of Reading, Reading RG6 6AX, UK

ARTICLE INFO

Article history:
Received 3 March 2009
Received in revised form 1 April 2009
Accepted 2 April 2009
Available online xxxx
Communicated by V.M. Agranovich

ABSTRACT

Recent experiments have demonstrated that nanoparticles which sparsely distributed over a solid substrate can substantially change the flow conditions at the solid surface in the presence of slip. Inspired by these observations, the flow past tiny particles seeded on a solid substrate is investigated theoretically in the framework of an interface formation model. It has been shown, that even a single seeded nanoparticle can reduce significantly the measurable tangential component of hydrodynamic velocity at the substrate and affect the amount of the observed apparent slippage of the liquid. The effect from the particle manifests in a form of a long relaxation tail defined by the characteristic time of the interface formation process. A comparison with experiments has demonstrated a good agreement between theoretically predicted and experimentally observed values of the relaxation tail length scale.

Capillary flows with forming interfaces occur universally in nature and in technology [1]. One of the central issues in quantitative description of this kind of flows is slippage of liquid at the solid surface [1–4]. For example, the amount of slip directly defines the dynamics of dewetting of thin liquid films and the contact angle in the process of dynamic wetting [2,3]. However, while the concept of slip has been widely accepted, quantitatively, there is still no consensus on the amount of slip [5–8]. The main factor, which may interfere with precise measurements and is often difficult to control in experiments, is the surface roughness. The effects of surface roughness on the flow conditions at solid surfaces have been studied theoretically, and experimentally, by several methods, such as macroscopic hydrodynamic and microscopic modelling, and mesoscopic analysis [5–18]. In this Letter, we consider one particular aspect of the phenomenon of slip on irregular surfaces, namely the influence of sparsely distributed nanoscale obstacles on the magnitude of slip, using a macroscopic approach. Our study is motivated, to a large extent, by the results of recent observations of slip [17,18], where the parameters of the surface roughness, such as the peak-to-valley difference and the distance between the asperities, were varied gradually on the nanoscale to quantify the amount of slip as a function of these parameters. Of particular interest are the results reported in [18], where the surface roughness had been progressively introduced by seeding single nanoparticles, of approximately uniform size, to specifically study the slip behaviour in the transient regime between smooth and rough surfaces.

Consider experimental results in [18] in more detail. The flow measurements of hexadecane at the initially molecularly smooth sapphire surfaces, covered with PDMS oligomer layer, have shown finite slip length λ approaching $\lambda \simeq 250 \pm 50$ nm. Then the same measurements have been taken on the surface modified with seeded small particles of 25–30 nm size. Remarkably, strong effect has been already observed with only 2% of the substrate area covered by the particles, i.e. when the average distance between the particles is about 180 nm. The slip length has shown a perceptible decline to $\lambda \simeq 150 \pm 50$ nm, whilst the average distance between the particles was still much greater than the particle size. Further increase of the area covered by the particles to just 5% was sufficient to decrease the observed slip length to $\lambda \simeq 50 \pm 50$ nm and thus, within the accuracy of measurements, to restore the no-slip condition. This effect has no satisfactory theoretical explanation so far, and one might assume that the particles were able to disturb the flow at the boundary on a length scale large compared to their own size. In order to identify the mechanisms of the phenomenon and bearing in mind that, as shown in [19], the effects of slip and the surface-tension gradients are coupled in the interfacial layer, we consider the interfacial dynamics as it could be affected by the presence of seeded particles. We will show that even a single seeded particle will disturb the interfacial layer and create surface tension gradients. This effect, generated by the seeded particles, is expected to be similar to the well-known Marangoni phenomenon, first discovered for the surface tension gradients induced by the gradients of surface temperature [20].

The mathematical model that we use here is based on the interface formation theory developed earlier [2], coupled with the effect of surface slip. In the case of a liquid consisting of spherical molecules, this effect, studied microscopically, has been shown to be sufficient to produce surface slip exceeding 30 molecular diameters [21,22]. To simplify the problem, consider a steady two-dimensional Stokes flow (in the vicinity of the substrate, one al-

E-mail address: a.lukyanov@reading.ac.uk.

0375-9601/$ – see front matter
doi:10.1016/j.physleta.2009.04.005

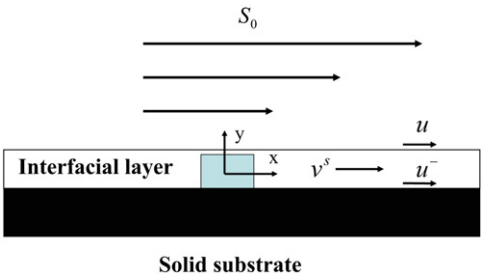

Fig. 1. Definition sketch for the problem.

most always has flows with negligible inertia) of an incompressible Newtonian liquid of constant density ρ and viscosity μ over a smooth solid surface with just one particle (with similar to the substrate physical properties) seeded on the surface. We note, however, that, geometrically, the three-dimensional analogue of the two-dimensional particle introduced here would be a lattice of threads lying on the surface normal to the direction of the flow. On the one hand, this simplification will allow us to obtain readily observed analytical results; on the other hand, this case is sufficiently representative to study the main features of the phenomenon.

The flow velocity $\mathbf{u}$ and pressure p in the bulk satisfy the Navier–Stokes (NS) equations,

$$\nabla \cdot \mathbf{u} = 0, \qquad \nabla p = \mu \nabla^2 \mathbf{u}. \tag{1}$$

The flow is driven by a plane-parallel constant shear S_0 in the far field. In the (x, y) plane of a Cartesian coordinate system, the origin of which is at the centre of the particle on the solid substrate, (Fig. 1), one has:

$$\frac{\partial u_x}{\partial y} = S_0, \qquad u_y = 0, \quad y \to \infty. \tag{2}$$

Boundary condition on the solid surface are given by [2]:

$$\mathbf{v}^s \cdot \mathbf{n} = 0, \tag{3}$$

$$\mu \mathbf{n} \cdot \left[\nabla \mathbf{u} + (\nabla \mathbf{u})^*\right] \cdot (\mathbf{I} - \mathbf{nn}) + \frac{1}{2}\nabla \sigma = \beta (\mathbf{u} - \mathbf{u}^-) \cdot (\mathbf{I} - \mathbf{nn}), \tag{4}$$

$$\rho \mathbf{u} \cdot \mathbf{n} = \left(\rho^s - \rho_e^s\right)\tau^{-1}, \tag{5}$$

$$\nabla \cdot \left(\rho^s \mathbf{v}^s\right) = -\left(\rho^s - \rho_e^s\right)\tau^{-1}, \tag{6}$$

$$\mathbf{v}^s \cdot (\mathbf{I} - \mathbf{nn}) = \frac{1}{2}(\mathbf{u} + \mathbf{u}^-) \cdot (\mathbf{I} - \mathbf{nn}) + \alpha \nabla \sigma, \tag{7}$$

$$\sigma = \gamma\left(\rho_0^s - \rho^s\right). \tag{8}$$

Here $\sigma = \gamma(\rho_0^s - \rho^s)$ is the surface tension in the interfacial layer which is modelled as a two-dimensional 'surface phase'; ρ^s is the surface density in this phase (mass per unit area) and $\mathbf{v}^s$ is the velocity with which it is transported along the interface; $\mathbf{u}^-$ is the velocity on the *solid*-facing side of the liquid–solid interfacial layer (Fig. 1); α, β, γ, τ, ρ_e^s and ρ_0^s are phenomenological material constants; $\mathbf{n}$ is the normal vector pointing in the liquid, $\mathbf{I}$ is the metric tensor; the tensor $(\mathbf{I} - \mathbf{nn})$ singles out the tangential projection of a vector; an asterisk marking a second-rank tensor indicates its transposition.

It should be emphasized here, that the above formulation can only be employed for lyophilic or, possibly, for intermediate liquid–solid combinations. In the opposite case of lyophobic combinations, the flow at the boundary may be conditioned by the trapped bubbles and the nature of the boundary conditions will be different. This is a special case and it is beyond the scope of the present analysis.

Conditions (3)–(8) have been obtained using methods of irreversible thermodynamics so that here we will only briefly comment on their meaning with more detail available in [2]. The

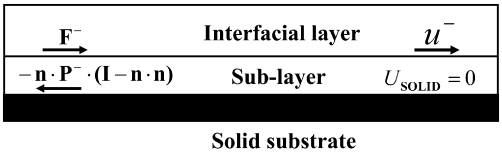

Fig. 2. Definition sketch for the problem to illustrate the *surface* slip condition (9).

model takes into account mass exchange between the bulk and the surface phase (5) that takes place when the surface density ρ^s deviates from its equilibrium value ρ_e^s. The parameter τ is the surface density and the surface tension relaxation time (the main parameter describing the interface formation). Importantly, the tangential components of the velocity in the surface phase $\mathbf{v}^s$, the bulk velocity evaluated on the *liquid*-facing side of the interface $\mathbf{u}$ and the velocity on the *solid*-facing side of the interface $\mathbf{u}^-$ are, in a general case, all different due to the torques acting on the surface phase. The conditions relating these components are given by (4) and (7). Constants α and β are characteristic parameters of the response of the interface to surface-tension gradients and the external torques. We will further use a simplifying assumption, to reduce the number of parameters, that $\alpha = \beta^{-1}$, see details in [2,23].

The problem formulation should be complemented by an equation for the velocity $\mathbf{u}^-$ on the *solid*-facing side of the interfacial layer. It is often assumed that the velocity $\mathbf{u}^-$ is equal to that of the solid, that is in our case $\mathbf{u}_\parallel^- = 0$, so that there is no *actual* slippage of the liquid on solid that would have been observed, for example, in molecular dynamics simulations. Potentially, however, it is possible that $\mathbf{u}_\parallel^- \neq 0$. For example, such surface slip has been directly observed in molecular dynamics simulations [22].

To account for this effect, by analogy with the generalised Navier condition (4), a relationship between $\mathbf{u}^-$ and the substrate velocity $(= 0)$ can be written in the form

$$\beta_s \mathbf{u}_\parallel^- = \mathbf{F}^-, \tag{9}$$

where the force $\mathbf{F}^- = \mathbf{n} \cdot \mathbf{P}^- \cdot (\mathbf{I} - \mathbf{nn})$ (Fig. 2), $\mathbf{P}^-$ is the stress tensor on the *solid*-facing side of the liquid–solid interface given by the momentum balance equation of the interfacial layer,

$$\mathbf{n} \cdot P^- \cdot (\mathbf{I} - \mathbf{nn}) = \mu \mathbf{n} \cdot \left[\nabla \mathbf{u} + (\nabla \mathbf{u})^*\right] \cdot (\mathbf{I} - \mathbf{nn}) + \nabla \sigma, \tag{10}$$

and β_s is a phenomenological parameter, similar to β. Note, that condition $\mathbf{u}_\parallel^- = 0$ is recovered from (9) at $\beta_s \to \infty$.

Condition (9) can be illustrated if we consider a sub-layer at the solid substrate (Fig. 2), which has essentially smaller length scale and different from the main interfacial layer properties, such as viscosity. Then (9) is obtained in a similar way as (4), but neglecting the surface tension effects in the sub-layer. Note, that a condition similar to (9) has been considered from mesoscopic and microscopic points of view, applying Green–Kubo relations, for a liquid consisting of spherical molecules and for a periodic substrate interacting with the fluid by means of Lennard-Jones potentials in [21,22].

Physically, the origin of this effect at the sub-layer may be either due to the true surface slip, directly observed in molecular dynamics simulations, or due to the ordered structure (reorientation of molecules) induced by the presence of solid wall resulting in the state with much lower viscosity [15,21,22,24–27]. The structure has been observed directly, by different techniques, in experiments and has been studied by mesoscopic analysis [15,24–27]. We will further refer to (9) as the *surface* slip condition at variance to the apparent slip, see further discussion.

The difference between the tangential components of $\mathbf{u}$ (i.e. the velocity on the *liquid*-facing side of the interface) and $\mathbf{u}^-$ can be referred to as 'apparent slip' that appears only in the macroscopic hydrodynamic modelling of interfaces. The notion of apparent slip

simply represents the fact that description of what is going on in the interfacial layer is below the spatial resolution of the NS model and hence, for the NS equations, the interfacial layer manifests itself only in terms of the boundary conditions on its *liquid*-facing side, in other words, the NS equations are not able to "observe" the solid surface directly. As a result, the macroscopic boundary conditions for the NS equations are to be specified on the *liquid*-facing side of the interface. The *surface* slip operates on smaller length scales and is obviously not associated with the interfacial surface tension effects.

In equilibrium (when $\rho^s = \rho_e^s$)

$$\mathbf{u}\cdot\mathbf{n} = 0$$

and

$$\left(\frac{\mu}{\beta} + \frac{\mu}{\beta_s}\right)\frac{\partial u_\parallel}{\partial n} = u_\parallel.$$

Identifying the slip length measured in experiments with

$$\lambda = \frac{\mu}{\beta} + \frac{\mu}{\beta_s},$$

we arrive at the form of the standard Navier boundary condition

$$\lambda\frac{\partial u_\parallel}{\partial n} = u_\parallel.$$

So, in equilibrium situations, the contributions from apparent and *surface* slip collapse into one parameter, the measurable slip length λ, so that it appears that surface slip is not directly observable. From this point of view, the split of the interfacial layer into two regions looks 'artificial'. But, as we will see later, once the equilibrium situation is disturbed by the seeded particles, the contribution from surface slip can be clearly observed.

Now, to account for the presence of particle, we introduce an additional condition at $x = 0$, $y = 0$, where the particle is located. To obtain informative asymptotic results, we apply a simplified condition, which is

$$v^s(0) = V_0, \tag{11}$$

where V_0 is a free parameter. This condition implies that the seeded particle can only change the liquid flux along the interfacial layer, but not the layer's geometry. This formulation is justified, if the seeded particle has the size of the order of the interfacial layer h, which is, according to experimental estimates [23,27], $h \sim 1$–5 nm. One needs to clarify here that the size of the interfacial layer h is not the actual parameter of the macroscopic model, where the interface has zero thickness. This fact is reflected in the nature of the boundary condition (11), which is specified at a point on the boundary.

Note, that the maximal value the parameter V_0 can take is, of course, proportional to the shear rate S_0. That is in equilibrium ($|x| \to \infty$), we have $V_0 = \bar{V}_0 S_0 \lambda$, where

$$0 \leqslant \bar{V}_0 \leqslant \frac{1}{2}\left(\frac{\lambda_a + 2\lambda_s}{\lambda_a + \lambda_s}\right),$$

$\lambda_s = \mu/\beta_s$ is *surface* slip length and $\lambda_a = \mu/\beta$ is apparent slip length.

It is now convenient to change to non-dimensional variables using $L = \lambda$, $U_0 = LS_0$, $p_0 = \frac{\mu U_0}{L}$ and ρ_e^s as scales for velocity, length, pressure and the surface density; $\lambda = \lambda_a + \lambda_s$ is, as before, the characteristic slip length. Then, the system of equations (1)–(10) takes the form

$$\nabla\cdot\mathbf{u} = 0, \qquad \nabla p = \nabla^2\mathbf{u}, \tag{12}$$

$$u_x = \left(\frac{\partial u_x}{\partial y} + \frac{\partial u_y}{\partial x}\right) - \frac{1}{2Ca}\frac{\partial \rho^s}{\partial x}\left(\frac{1+2\delta_s}{1+\delta_s}\right), \tag{13}$$

$$\epsilon u_y = Q\left(\rho^s - 1\right), \tag{14}$$

$$\epsilon\frac{\partial \rho^s v^s}{\partial x} = 1 - \rho^s, \tag{15}$$

$$2v^s = u_x + \frac{\delta_s}{1+\delta_s}\left(\frac{\partial u_x}{\partial y} + \frac{\partial u_y}{\partial x}\right) - \frac{1}{Ca}\frac{\partial \rho^s}{\partial x}\left(\frac{2+\delta_s}{1+\delta_s}\right). \tag{16}$$

To complete the problem formulation, we add conditions (2), (11) and assume that far away from the particle the surface density tends to its equilibrium value,

$$\frac{\partial u_x}{\partial y} \to 1, \qquad u_y \to 0, \quad x, y \to \infty, \tag{17}$$

$$v^s = \bar{V}_0, \quad x = 0, \tag{18}$$

$$\rho^s \to 1, \quad |x| \to \infty. \tag{19}$$

The problem has five non-dimensional parameters $\epsilon = \frac{U_0\tau}{\lambda}$, $Ca = \frac{\mu U_0}{\sigma_0}$, $Q = \frac{\rho_e^s}{\rho\lambda}$, $\delta_s = \beta/\beta_s$ and $\bar{V}_0$; parameter $\sigma_0 = \gamma\rho_e^s$ is the characteristic surface tension, γ is inversely proportional to the fluid's compressibility and is, roughly, the square of the speed of sound; $\rho_e^s \sim \rho_0^s \simeq \rho h$. Parameter ϵ is the ratio of the characteristic relaxation length $U_0\tau$ to the characteristic slip length λ, Ca is the capillary number, parameter $Q \simeq h/\lambda$ characterizes the mass flux into/out of the liquid–solid interface, parameter δ_s is the ratio of the *surface* slip length $\lambda_s = \mu/\beta_s$ to the apparent slip length $\lambda_a = \mu/\beta$, $\delta_s = \lambda_s/\lambda_a$ and parameter $\bar{V}_0$ characterizes the strength of the interaction between the seeded particle and the flux in the interfacial layer (if $\bar{V}_0 = 0$ then the particle completely blocks the flux in the interfacial layer).

There are three small parameters in the system; Ca, ϵ and Q. Taking $S_0 \sim 10^4$ s^{-1}, $\lambda \sim 100$ nm, $\sigma_0 \sim 10^{-1}$ N/m ($\rho_e^s \sim 10^{-6}$ kg/m^2, $\gamma \sim 10^5$ m^2/s^2), $\mu \sim 10^{-3}$ Pa s, $\tau \sim 10^{-8}$ s as estimates of the characteristic shear rate, slip length, surface tension, viscosity and relaxation time, $U_0 \sim 10^{-3}$ m/s and $Ca \sim 10^{-5}$, $\epsilon \sim 10^{-4}$, $Q \sim 3\times 10^{-2}$. Here, parameter τ is taken, according to the estimates obtained from experiments on dynamic wetting [23], to scale for simple fluids as $\tau = 10^{-8}(\frac{\mu}{1\text{ mPa s}})$ s. Note, that the Reynolds number, in this case, $Re = \rho U_0\lambda/\mu \simeq 10^{-4} \ll 1$ and the use of the Stokes approximation is well justified.

The asymptotic solution to (12)–(19) in the limit $\epsilon \to 0$, $Ca \to 0$ and $Q \to 0$ has been obtained using matching asymptotic expansion technique, assuming the following order of the small parameters $\epsilon/Ca \sim O(1)$ and $\epsilon/Q \sim O(\epsilon)$. There are three asymptotic regions at $\epsilon \to 0$; the inner region $|x| \sim \epsilon$, the intermediate region $|x| \sim 1$ and the outer region $|x| \gg 1$. Matching asymptotic expansions in all three regions, one can obtain, in the leading order, at the boundary $y = 0$,

$$\rho^s(x) = 1 \mp \epsilon\xi_0 C_\delta \exp\left(-\xi_0|x|\right), \tag{20}$$

$$v^s(x) = v_0^s - C_\delta \exp\left(-\xi_0|x|\right), \tag{21}$$

$$u_x(x,0) = 1 - \frac{2+4\delta_s}{5+4\delta_s}C_\delta \exp\left(-\xi_0|x|\right), \tag{22}$$

$$u_y(x,0) = \mp Q\,\xi_0 C_\delta \exp\left(-\xi_0|x|\right), \tag{23}$$

where

$$\xi_0^2 = \frac{Ca}{\epsilon}\frac{1+\delta_s}{\frac{5}{4}+\delta_s}, \qquad v_0^s = \frac{1}{2}\left(1 + \frac{\delta_s}{1+\delta_s}\right), \qquad C_\delta = v_0^s - \bar{V}_0, \tag{24}$$

and the upper sign is for $x > 0$. Note, that to obtain the simplest and readily observable analytic expressions, we have neglected contributions proportional to $Q \ll 1$ in the coefficients of the asymptotic solution (20)–(22) and used a simplifying assumption that numerically parameter $\xi_0^2 \ll 1$. In this case, the boundary conditions describing surface distributions (13)–(16) become effectively decoupled from the driving bulk shear flow (12), and one

can show that in the leading order $\frac{\partial u_x}{\partial y} \approx 1$. It is interesting to note that numerical solution of system (12)–(19) has shown that the obtained asymptotic expressions (20)–(22) can well be used even at $\xi_0^2 \sim 1$ to approximate the solution.

As is seen from distributions (20)–(23), the surface density is, as it is expected for low compressible medium, only slightly perturbed by the seeded particle, $\Delta\rho^s \sim O(\epsilon)$, but, this perturbation is sufficient to create essential changes in the velocity field u_x at the boundary. The effect is maximal at $\delta_s \to \infty$ ($\beta_s \to 0$), when large *surface* slip occurs at the solid substrate, and at $\bar{V}_0 = 0$, when the seeded particle totally blocks the flux in the interfacial layer. In this limit, the (measurable) hydrodynamic velocity at the location of the particle tends to the value defined by the apparent slip only,

$$u_x(0,0) = 1 - \frac{2+4\delta_s}{5+4\delta_s} C_\delta,$$

$$u_x(0,0) \to \frac{5}{4\delta_s} + O\left(\frac{1}{\delta_s^2}\right), \quad \delta_s \to \infty.$$

Away from the particle, the velocity recovers to its undisturbed value $u_x(\pm\infty, 0) = 1$ over the distance defined by $l_0 = \xi_0^{-1} \gg 1$. In the opposite case, $\delta_s \to 0$ ($\beta_s \to \infty$), i.e. when the slip is mostly apparent, the maximal velocity reduction, at $\bar{V}_0 = 0$, is 20% of the undisturbed value,

$$u_x(0,0) \to \frac{4}{5}, \quad \delta_s \to 0.$$

The mechanism of this effect in both cases is the same. While the seeded particle directly affects only the surface velocity, via the condition $v^s(0) = \bar{V}_0$, this disturbs the equilibrium state of the surface density $\rho^s = 1$ and the process of *interface formation* takes off; the fluid in the interface is slightly compressed, $\rho^s > 1$, while it is driven by the outer flow towards the particle and is rarefied, while it is driven away from the particle, $\rho^s < 1$. The resulting surface density gradient, the particle induced Marangoni effect, in turn, creates gradient of the surface tension thus disturbing the force balance in the interfacial layer, Eq. (10). As a result, the tangential stresses acting on both sides of the interfacial layer are adjusted to preserve the balance of forces and at the same time changing the (measurable) hydrodynamic velocity u_x. As is seen from (10), the effect is expected to be stronger at $\beta_s \to 0$, since in this case $\mathbf{P}^- \to 0$ and the induced surface tension gradient is only balanced by the tangential stress on the *liquid*-facing side of the interface, while in the opposite limit, the induced surface tension is redistributed between the two sides of the interface.

It is important that in the model the maximal reduction of the tangential velocity at the substrate, as is seen from (22), is limited by the monotonically increasing function of one parameter δ_s which is the ratio λ_s/λ_a,

$$\max|\Delta u_x| \leqslant (1+2\delta_s)^2(5+4\delta_s)^{-1}(1+\delta_s)^{-1}.$$

Thus, macroscopic measurements of this velocity variation can be potentially used to identify the presence of *surface* slip. For example, in [18], $\min(\lambda) \leqslant 50$ nm according to the accuracy of measurements (this estimate is quantitatively consistent with the slip length of hexadecane, of the order of 30 nm, measured independently in [28]), then $0.8 \leqslant \max|\Delta u_x|$ and $4.5 \leqslant \delta_s$, so that large *surface* slip occurs.

Now consider the transition region l_0. If we revert to the dimensional length scale $\hat{l}_0 = \lambda l_0$ then

$$\hat{l}_0 = \sqrt{\lambda^2 \frac{\epsilon}{Ca} \frac{(\frac{5}{4}+\delta_s)}{(1+\delta_s)}} \simeq \sqrt{\frac{\lambda\tau\sigma_0}{\mu}}. \tag{25}$$

What is this characteristic distance? If we use experimental parameters from [18], i.e. $\lambda \simeq 250$ nm, $\mu \simeq 3\times10^{-3}$ Pa s, $\sigma_0 \simeq$ 3×10^{-2} N/m and $\tau \simeq 3\times10^{-8}$ s, then $\hat{l}_0 \simeq 270$ nm which is close to $\hat{l}_0 \simeq 180$ nm experimentally observed. Some discrepancy in this case is actually expected if we note that, geometrically, the two-dimensional analogue of the one-dimensional model presented here would be a lattice of grid lines instead of single seeded particles, and thus the whole effect is to be stronger.

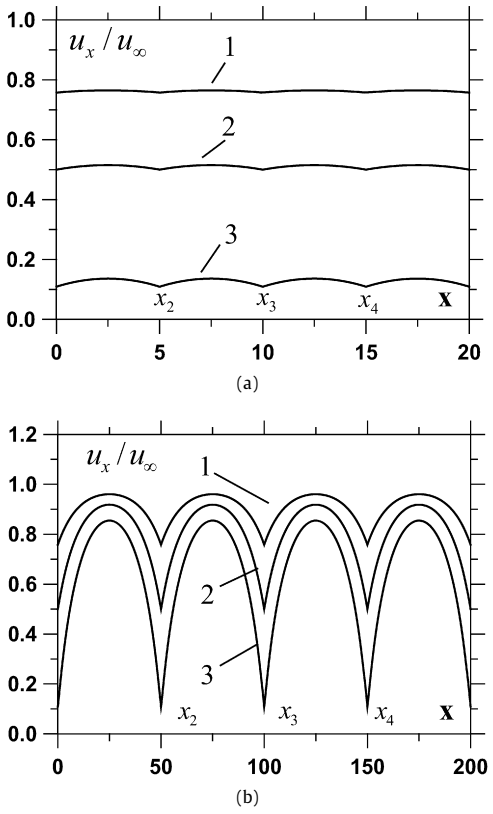

Fig. 3. Distributions of the tangential component of the bulk velocity on the *liquid*-facing side of the interfacial layer u_x along the substrate at different values of parameter δ_s and the distance between the particles Δx distributed uniformly; (a) $|\Delta x| = 5$, (b) $|\Delta x| = 50$. The seeded particles are located at x_i, $i = 1, \ldots, 5$. For all curves $l_0 = 10$ and $\bar{V}_0 = 0$; (1) $\delta_s = 0.1$, (2) $\delta_s = 1$, (3) $\delta_s = 10$; the distance x along the substrate is scaled with the slip length λ and u_x is scaled with the undisturbed value of the velocity, far away from the seeded particles, u_∞.

Remarkably, the characteristic (measurable) distance $\hat{l}_0$, (25), depends on, apart from the usually known parameters σ_0, μ and the measurable slip length λ, the characteristic relaxation time τ of the surface phase – the parameter which is central to the interface formation process, but which has been, so far, only evaluated indirectly from experiments on dynamic wetting [23]. Now, slip measurements on patterned substrates provide an alternative and unique method of direct measurements of this fundamental parameter.

The analysis can be easily generalised to the case of several particles located at points x_k, $k = 1, \ldots, N$. The asymptotic distribution, similar to (20)–(22), of the flow field at the boundary between each pair of the particles located, say, at x_1 and x_2, is given by

$$u_x(x,0) = 1 - \big(A\exp(-\xi_0 x) + B\exp(\xi_0 x)\big)\frac{2+4\delta_s}{5+4\delta_s},$$

$$A = B\exp\big(\xi_0(x_1+x_2)\big), \qquad B = \frac{v_0^s - \bar{V}_0}{\exp(\xi_0 x_1) + \exp(\xi_0 x_2)}. \tag{26}$$

This solution is illustrated in Fig. 3 at $\bar{V}_0 = 0$ for different values of parameter δ_s and the distance between the particles. It is seen, that

when the distance between the particles is less then the characteristic length l_0 then the tangential component of the bulk velocity at the interface is reduced, by the seeded particles, to the value defined by the apparent slip length λ_a. The *surface* slip length, λ_s, will only manifest itself if the distance between the particles Δx would be much larger than l_0, in particular, for the experiment with hexadecane [18], $\Delta x \gg l_0 \simeq 270$ nm. This outcome is qualitatively consistent with the conclusions drawn in [8] and the trend observed in molecular dynamics simulations [29].

In conclusion, our analysis predicts that even a single nanoparticle seeded on the solid surface can result in significant effect on the observable slip length and on the boundary conditions at the solid substrates. This sensitivity of the slip effect to the surface irregularities may be an explanation for the at times contradictory reports on the slip length measurements. Importantly, the predicted effect reflects the rate of interface formation and can be used to determine the dynamical characteristic of the surface phase – its relaxation time. The outcome of the theoretical analysis, presented here, is crucial for interpretation of slip length measurements and can be potentially used to identify the appearance of surface slip and in the design of future experiments.

References

[1] T.M. Squires, S.R. Quake, Rev. Mod. Phys. 77 (7) (2005) 977.
[2] Y.D. Shikhmurzaev, Capillary Flows with Forming Interfaces, Taylor & Francis, 2007.
[3] R. Fetzer, K. Jacobs, Langmuir 23 (2007) 11617.
[4] L. Bocquet, J.L. Barrat, Soft Matter 3 (2007) 685.
[5] R. Pit, H. Hervet, L. Leger, Phys. Rev. Lett. 85 (2000) 980.
[6] E. Bonaccurso, H.J. But, V.S.J. Craig, Phys. Rev. Lett. 90 (2003) 144501.
[7] B. Cross, A. Steinberger, C. Cottin-Bizonne, J.P. Rieu, E. Charlaix, Europhys. Lett. 73 (2006) 390.
[8] O.I. Vinogradova, G. Yakubov, Phys. Rev. E 73 (2006) 045302.
[9] S. Richardson, J. Fluid Mech. 59 (1973) 707.
[10] I.V. Ponomarev, A.E. Meyerovich, Phys. Rev. E 67 (2003) 026302.
[11] R. Krechetnikov, G.M. Homsy, Phys. Fluids 17 (2005) 102108.
[12] C.Y. Wang, Phys. Fluids 15 (2003) 1114.
[13] N.V. Priezjev, S.M. Troian, J. Fluid Mech. 554 (2006) 25.
[14] N.V. Priezjev, A.A. Darhuber, S.M. Troian, Phys. Rev. E 71 (2005) 041608.
[15] L. Biferale, et al., J. Comput.-Aided Mater. Des. 14 (2007) 447.
[16] R. Benzi, et al., J. Fluid Mech. 548 (2006) 257.
[17] Y. Zhu, S. Granick, Phys. Rev. Lett. 88 (2002) 106102.
[18] T. Schmatko, H. Hervet, L. Leger, Langmuir 22 (2006) 6843.
[19] J.E. Sprittles, Y.D. Shikhmurzaev, Phys. Rev. E 76 (2007) 021602.
[20] C. Marangoni, P. Stefanelli, Nuovo Cimento Ser. 2 7–8 (1872) 301.
[21] L. Bocquet, J.L. Barrat, Phys. Rev. E 49 (1994) 3079.
[22] J.L. Barrat, L. Bocquet, Phys. Rev. Lett. 82 (1999) 4671.
[23] T.D. Blake, Y.D. Shikhmurzaev, J. Colloid Interface Sci. 253 (2002) 196.
[24] M. Grosse-Rhode, G.H. Findenegg, J. Colloid Interface Sci. 64 (1978) 374.
[25] B.V. Derjaguin, V.V. Karasev, Russian Chem. Rev. 57 (1988) 634.
[26] C.J. Yu, A.G. Richter, J. Kmetko, A. Datta, P. Dutta, Phys. Rev. E 63 (2001) 021205.
[27] B.V. Derjaguin, N.V. Churaev, V.M. Muller, Surface Forces, Consultants Bureau, New York, 1987.
[28] J.T. Cheng, N. Giordano, Phys. Rev. E 65 (2002) 031206.
[29] A. Jabbarzadeh, J.D. Atkinson, R.I. Tanner, Phys. Rev. E 61 (2000) 690.

Please cite this article in press as: A.V. Lukyanov, Physics Letters A (2009), doi:10.1016/j.physleta.2009.04.005